JOURNAL OF APPLIED ELECTROCHEMISTRY 12 (1982) 171–183

The breakdown of PbO_2–Ti anodes

D. GILROY

The Electricity Council Research Centre, Capenhurst, Chester, UK

Received 23 June 1981

Lead dioxide–titanium electrodes have been tested as oxygen evolving anodes in 1 mol dm^{-3} H_2SO_4, at high current densities. Three modes of failure, shedding, thinning and deactivation have been identified. The first two are the result of stresses produced during electrodeposition, compounded by the thermal effects of polarization. Some improvements in these aspects of performance have been made by manipulation of the plating conditions. Deactivation has been modelled by considering the diffusion of special sites from the bulk material. There is continuous redeposition of PbO_2 from the solution.

1. Introduction

Experimental work on the electrodeposition of lead dioxide on titanium substrates has been reported previously [1]. Here the utilization of such electrodes as oxygen evolving anodes in 1 mol dm^{-3} H_2SO_4, at high current density, has been investigated.

2. Experimental details

2.1. *Electrode preparation*

The substrates were accurately cut from a 2 mm titanium sheet (IMI grade 115) as 100 mm × 10 mm plates. The surfaces were prepared by blasting with alumina particles followed by ultra sonic cleaning [2]. A batch of six electrodes was clamped to a horizontal titanium current feeder bar, and the assembly was masked with lacquer to leave an active area of 80 mm × 10 mm on one side only of each electrode. Plating was carried out in a lead nitrate/nitric acid solution containing copper nitrate as a cathodic depolarizing agent. Preliminary experiments established that the presence of Cu^{2+} ions had no effect on the current transients for lead dioxide deposition. Anodic coatings, normally of 100 C cm^{-2}, were formed potentiostatically as before [1], using a PbO_2 reference electrode. After plating the electrodes were rinsed in distilled water, dried in air and stored in a dry box. All lacquer was removed before use.

2.2. *Electrode testing cell*

The electrodes were used as oxygen evolving anodes in 1 mol dm^{-3} H_2SO_4 solution, under potentiostatic conditions. The perspex cell, in the form of a 50 mm × 20 mm rectangular channel, had an entry length of 550 mm and an exit length of 250 mm. An electrode fitted closely into a groove machined from one of the wider sides of the cell in such a way that the PbO_2 surface was flush with the channel. An active area of 50 mm × 10 mm was exposed to the solution, which flowed vertically parallel to the 10 mm dimension of the electrode. In many respects the cell arrangement was similar to that used by Pickett and Ong [3], and the hydrodynamic parameters of the present experiments may be calculated by reference to their work. An electrode was sealed into place with an 'o'-ring and stuffing box, and electrical contact was facilitated by painting the external surfaces with silver paint before attaching the current carrying lead. A compartment for a mercury/mercury sulphate reference electrode was bolted onto the cell behind the working electrode. The Luggin capillary was formed by drilling a 0.5 mm diameter hole through the titanium substrate before the electrodeposition of PbO_2. A 50 mm × 100 mm titanium counter electrode was fitted into the channel wall opposite the working electrode.

2.3. *Procedure*

A solution flow rate of 0.5 m s^{-1} was established

0021–891X/82/020171–13$03.30/0

in the cell using a total electrolyte volume of 150 dm^3. An electrode was first conditioned for 30 min at an anodic current density of 10 mA cm^{-2} then an initial polarization curve was determined by altering the potential in small increments (25 or 50 m V) from a starting point of about 1.2 V, noting the current at the end of each step. Potentials throughout are referred to the mecury/mercury sulphate electrode, in the presence of 1 mol dm^{-3} SO_4^{2-} ions.)

Electrode performance was assessed by following the current decay at constant potential. Several variables, including anode potential, cell current and temperature were monitored at appropriate intervals. Initial current densities were high, between 0.2 and 1.6 A cm^{-2}, and potential instability, due to the accumulation of gas bubbles in the Luggin capillary, could be present. At the end of an experiment some electrodes behaved as though passivation of the titanium substrate had occurred (i.e. the observed current depended on the current range selected on the potentiostat, as though additional resistance had been introduced into the circuit).

In some cases weight losses during polarization were monitored by removing the electrode at intervals from the cell, rinsing, drying and weighing before re-insertion. It was established that the handling procedure did not result in any significant loss of material.

2.4. *Structural examination*

Massive shedding of material in the above type of experiment was recorded by photographing some specimens after each removal from the cell. Other electrodes were examined at the end of polarization by mounting small portions (10 mm x 10 mm approximately) onto aluminium specimen stubs before insertion into the scanning electron microscope (Cambridge 180). Structural changes at both PbO_2 interfaces, and phenomena associated with the shedding of material could then be assessed.

3. Oxygen evolution

A summary of the initial polarization curves is presented in Fig. 1. At any given potential the mean of the logarithm of the total current (on

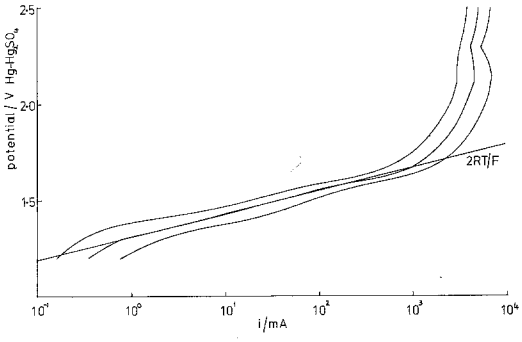

Fig. 1. Summary of initial polarization curves, showing the mean and unit standard deviations of log i at given potentials.

5 cm^2) has been calculated for 47 different electrodes. Unit standard deviations from the mean are also shown to indicate the reproducibility of the results. The calculations include batches of six electrodes each plated to give thicknesses corresponding to 10, 20 and 50 C cm^{-2}, as opposed to the normal value of 100 C cm^{-2}. Also included are data from 13 electrodes plated in the presence of cetyl tri-methyl ammonium bromide (CTAB). These variations produced no apparent trends in the polarization behaviour, but samples plated in the presence of added sodium acetate were somewhat more active, especially at the lower potentials, although the lifetimes were shorter. The acetate specimens are not included in Fig. 1.

For reference purposes a Tafel line of slope $(2RT/F)$ ($T = 20°$ C) has been drawn through the data, although it should be emphasized that this does not have too much significance when the behaviour of individual polarization curves is considered. Usually any Tafel regions are of limited extent and there is often a region at about 1.5 V where the current may decrease slightly with increasing potential before resuming the normal dependency. This suggests that some phase change may be occurring. Above this anomaly the Tafel slope may be less than $(2RT/F)$. At the highest potentials, ohmic drop becomes important but the curves have not been corrected for this.

The data are similar to those of oxygen evolution on lead anodes summarized by Kuhn [4].

4. Shedding

Examination of specimens after utilization shows the presence of three types of structural alteration:

shedding, thinning and redeposition. Most of the electrodes prepared by plating at room temperature from the normal bath, are subject to shedding, either during the recording of the polarization curve, or during the first few hours of testing. Pieces of lead dioxide, roughly circular in shape, are removed to leave vertical-sided holes with complete or partial exposure of the titanium at the base. The morphology of the failures is a consequence of the structure of the deposit, which was discussed in the previous paper [1]. After the initial nucleation at discrete centres, columnar crystals radiate outwards in all directions, so that, in the region adjacent to the substrate, growth is orientated parallel to the interface, until overlap is complete. As the film thickens, the columns assume a predominantly perpendicular aspect with respect to the interface. If the structure is most easily fractured between, rather than across, columns, then the observed hole shapes are readily explained. The micrographs of Fig. 2 illustrate the various features. Figs. 2a and b show, for example, 'rosette' formations of lead dioxide crystallites radiating outwards from nuclei among the debris on the floor of a cavity.

The dimensions of various holes in the direction parallel to the shorter side of the electrode were determined from photographs, micrographs or by direct measurement. Careful measurement of the 'hole diameters', defined in this way, of specimens removed from the cell at intervals during testing, showed no enlargement with time, although fresh holes might appear. Size distributions are presented, as before [1], by numbering the N holes in a sample $1, 2, 3 \ldots n_d \ldots N$, in the order of increasing diameters, d, and plotting n_d/N as a function of d. A typical result is given in Fig. 3. Throughout the thickness range from 10 to 100 μm, log-normal, as opposed to normal, distributions provide the more satisfactory representation of the data. In the summary diagram (Fig. 4) the curve for 100 μm deposits is a composite of six specimens, since the number of holes on an individual electrode is small, but the other curves refer to single specimens. A distribution of the diameters of nuclei, taken from the previous paper, for a situation in which overlap was essentially complete, is included. This suggests that in a 10 μm layer each hole corresponds to the shedding of a few nuclei only. Hole diameters, and numbers per unit area, depend on the lead dioxide thickness (see Fig. 5).

The above observations, describing failures which are obviously mechanical in nature, may be discussed by considering the stress, σ, present in a layer during formation and subsequent testing. Pangarov and Pangarova [5] have recently published a treatment of electrodeposition stress suggesting that it arises as a result of the departures from equilibrium shapes of the growing crystals. General equations, for single layers and for composite layers, were derived relating the stress to the layer thickness, l, in the following manner

$$\sigma = Kl^{-m} \tag{1}$$

where K is a combination of physical constants and m is a constant dependent on the growth model. For example, before overlap, during the formation of a single layer of crystals, with fast growth parallel to the substrate, $m \to 3/4$. In a multi-layer structure, if the crystals have similar dimensions in each layer, $m \to 0$, but at the other extreme $m \to 3/2$ when the deposit grows outwards as one layer only. Experimental results obtained by Udupa's group [6–8] and by Bushrod and Hampson [9], besides demonstrating the existence of stress in lead dioxide layers, usually show that the stress decays with time or thickness in agreement with Equation 1.

In some cases the electrodeposition stress alone may be sufficient to crack the film, as reported by Kuhn and Lartey [10], for example, but failure becomes much more likely when thermal stress, arising from the passage of high currents, is superimposed. Because of the mismatch with the substrate, and bearing in mind the orientations of crystallites in the layer, as described before, cracks will be preferentially initiated in the material adjacent to the titanium, and will spread outwards in all directions parallel to the interface. As a result, roughly circular plates of lead dioxide detached at the bases but fixed at the edges will be formed. The plates will fail by buckling when their diameters, d, have increased sufficiently to conform to a relation of the type given by Roark [11]

$$\sigma = k_1 \frac{E}{1-\nu^2}\left(\frac{l}{d}\right)^2. \tag{2}$$

This particular equation represents the critical

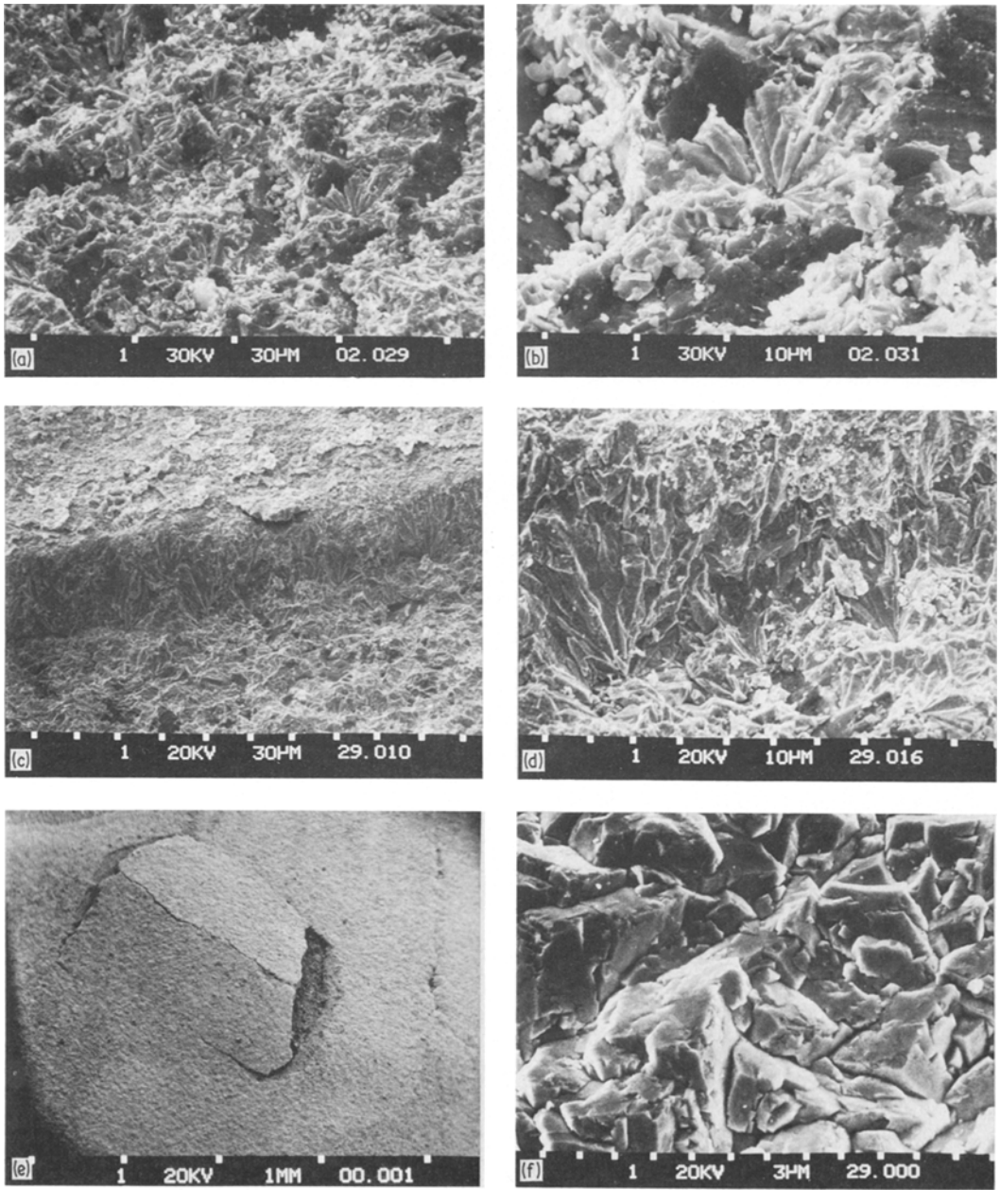

Fig. 2. Micrographs of PbO_2 deposits illustrating various features: (a, b) Debris left on the substrate after hole formation. 'Rosette' formations of crystallites radiating outwards from the original nuclei can be seen. Dark areas are exposed titanium. (c, d) Sides of holes illustrating the vertical rupture. Original nuclei are again visible. Undermining also occurs. (e) Hole formation showing buckling failure before material is completely shed. (f) Surface of unused PbO_2 layer consisting of pyramidal blocks. (g) Redeposition on the upper surface of PbO_2 during testing. The deposits are amorphous and the angular nature of the surface shown in Fig. 2f has been lost. (h) Dendritic redeposition on the floor of a hole. (i, j) Spherical nuclei formed on the titanium substrate by redeposition after substantial thinning. (k) Lead sulphate crystals formed on a partially detached portion of the PbO_2 layer.

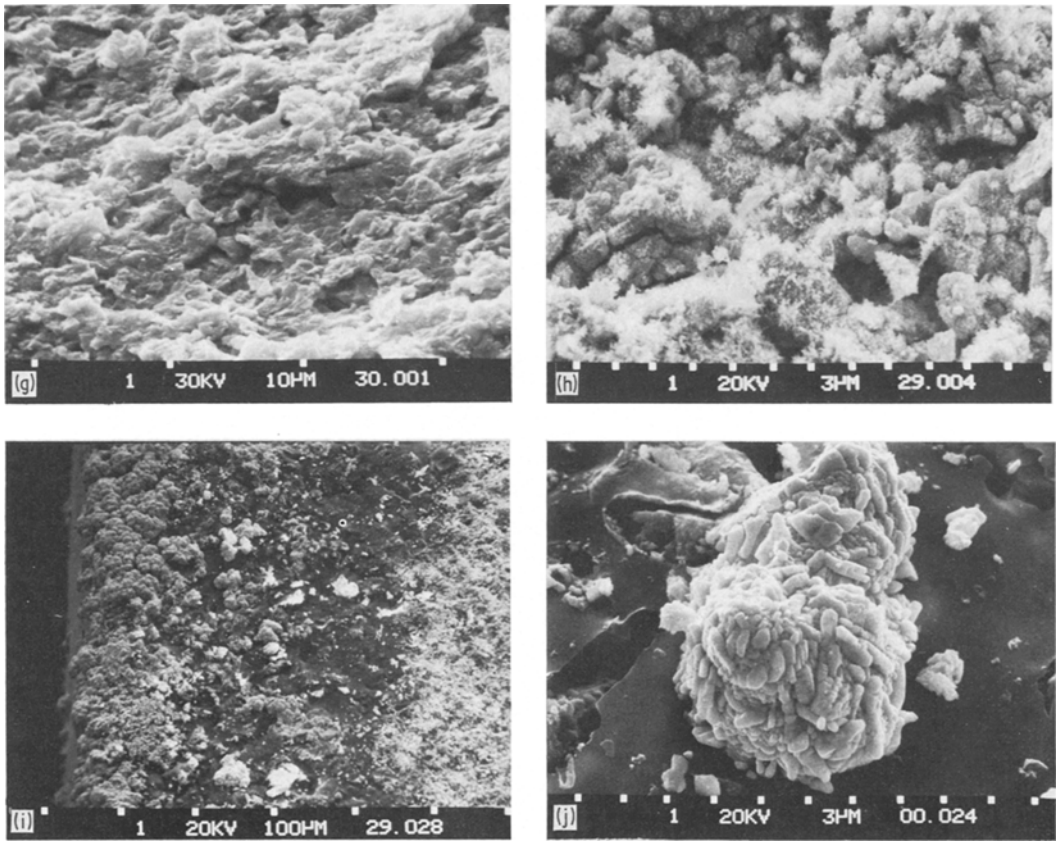

Fig. 2. Continued.

stress required to buckle a circular plate of diameter, d, and thickness, l with Young's modulus, E, and Poisson's ratio, ν. The plate is clamped at the edges and subjected to a radial compressive stress. Alternative models of this type of situation involve the same dependence of σ on $(l/d)^2$. Taking logarithms and differentiating gives

$$\frac{\mathrm{d}\log d}{\mathrm{d}\log l} = (1-\tfrac{1}{2})\frac{\mathrm{d}\log \sigma}{\mathrm{d}\log l}. \qquad (3)$$

The incidence of holes, N cm^{-2}, may also be approached by considering that the stress energy is relieved by the formation of new surface with energy γ cm^{-2}. For unit area of electrode the following expressions for the two quantities may be written

$$\text{Total surface energy} = 2\gamma N \frac{\pi d^2}{4}\left(1+\frac{4l}{d}\right) \qquad (4)$$

and

$$\text{Total stress energy} = \tfrac{1}{2}\frac{\sigma^2}{E} l. \qquad (5)$$

If a constant fraction of the stress energy is relieved one obtains

$$Nd^2\left(1+\frac{4l}{d}\right) = k_2 l\sigma^2 \qquad (6)$$

and using Equation 2

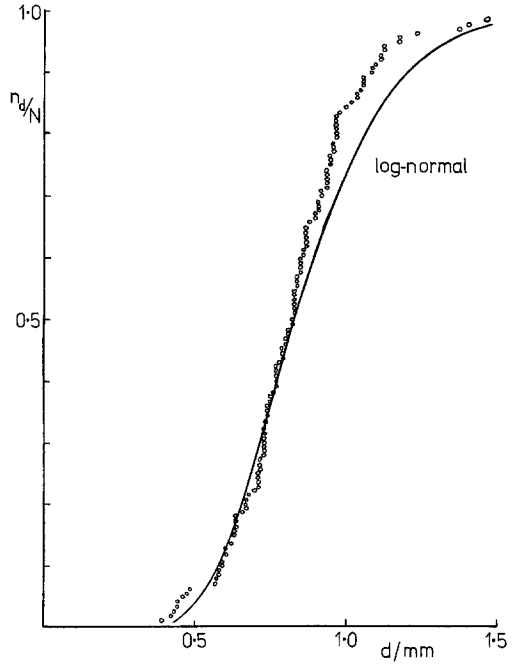

Fig. 3. Distribution of hole sizes on specimen 58 Layer thickness ~ 50 μm.

$$Nl\left(1+\frac{4l}{d}\right) = k_3\sigma^3 \qquad (7)$$

where k_2 and k_3 are constants. Again by taking logarithms and differentiating, and neglecting the variation of the term in brackets, one has approximately

$$\frac{\mathrm{d}\log N}{\mathrm{d}\log l} = -1 + 3\frac{\mathrm{d}\log\sigma}{\mathrm{d}\log l}. \qquad (8)$$

The stress, σ, is the summation of the electrodeposition stress and the thermal stress, and the latter arises mainly from the presence of reaction

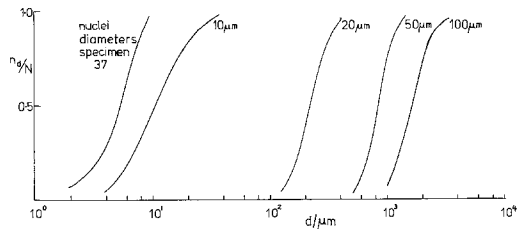

Fig. 4. Summary of hole size distributions as a function of layer thickness. A distribution of diameters of nuclei just before overlap, from the previous paper [1], has been included.

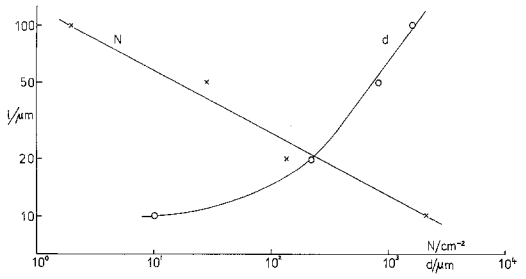

Fig. 5. Hole diameters, d, and numbers per unit area, N, as a function of layer thickness, l.

resistance at the solution interface. Since the initial conditions of testing are usually constant (i.e. current density = 1.4 A cm^{-2}, overvoltage ≃ 2.5 V), then a constant temperature rise ΔT at the surface may be assumed. It has been shown [11, 12] that the stresses produced in plates clamped at the edges and subjected to a temperature increase at one face are independent of thickness, and therefore any variation in $\mathrm{d}\log\sigma/\mathrm{d}\log l$ will be due solely to the effect of film thickness on electrodeposition stress. Experimentally, as shown in Fig. 5.

$$\frac{\mathrm{d}\log d}{\mathrm{d}\log l} = 1.3,$$

and

$$\frac{\mathrm{d}\log N}{\mathrm{d}\log l} = -3.1.$$

The value of

$$\frac{\mathrm{d}\log\sigma}{\mathrm{d}\log l} = -0.7$$

makes these results consistent with Equations 3 and 8. Furthermore, this value is also satisfactory when considered in terms of Equation 1 and the structure of the lead dioxide layer.

In summary the proposed shedding model is as follows:

1. The combination of thermal and electrodeposition stress produces cracks in the weakest part of the lead dioxide layer adjacent to the substrate.

2. The cracks propagate parallel to the interface so that a plate is separated.

3. When a plate reaches a critical diameter it fails by buckling. An example of a failure just

before material is shed is shown in the micrograph of Fig. 2e.

The model represents the data fairly well at the highest oxide thicknesses used here, but some departures are observed in specimens with 10 μm layers, probably for the following reasons.

(a) The buckling equation does not apply strictly when l/d is too large.

(b) Variation of the bracketed term in Equation 6 may become significant.

(c) The holes may have some lower limiting diameter corresponding to the removal of material corresponding to a single nucleus, as implied earlier.

Finally it may be noticed that crack propagation parallel to the interface must proceed easily after initiation, otherwise the lead dioxide layers would be undermined with many holes of sub-critical size, and electrode activity would be significantly impaired.

5. Stress relief

Previous workers have suggested that the electrodeposition stress in lead dioxide may be reduced by adding various compounds to the plating solution, and two of these additives were briefly investigated here. Other methods of achieving the same objective, including temperature and current density manipulation were also tried.

5.1. *Sodium acetate*

Sodium acetate [7] was added to the normal plating solution at room temperature to give concentrations between 0.02 and 0.5 mol dm^{-3}. The potential was adjusted to give final current densities of about 20 mA cm^{-2}. At the highest concentration the prepared electrodes were blistered upon removal from the plating bath, and failed rapidly during testing, although it may be pointed out that the pH of the bath was increased by this level of addition. Even though the polarization curves taken initially showed some increase in activity for oxygen evolution, material losses by shedding occurred in the early stages of testing, and the lifetimes of all the specimens were reduced when compared with the controls.

Hence the use of acetate is not recommended.

5.2. *CTAB*

Following suggestions put forward by Udupa's group [6, 8] additions of CTAB in concentrations between 10^{-4} and 5×10^{-3} mol dm^{-3} were made. To dissolve the material over most of this range it was necessary to raise the bath temperature to 60° C and later investigation showed that this factor alone was sufficient to prevent the formation of holes during subsequent anodic polarization. The specimens did, however, thin uniformly throughout the tests and quite high losses of material were recorded before failure. This aspect of electrode behaviour will be discussed later. Increasing the CTAB levels in the plating bath produced no extra benefit as far as lifetimes were concerned, and the use of elevated temperature was considered to be the predominant factor. The presence of the organic compound inhibited the electrodeposition, as expected, and plating potentials had to be increased significantly to initiate nucleation.

5.3. *Current density*

According to the previously discussed theory, stress should be minimized by carrying out electrodeposition under conditions as close to equilibrium as possible, implying the use of low current densities. This approach was investigated with a 60° C plating temperature to avoid the shedding phenomenon. Control specimens formed at the usual final current density of 20 mA cm^{-2} were compared with additional electrodes plated at 200 and 4 mA cm^{-2}. When tested potentiostatically the lifetimes increased marginally as the current density of formation decreased. In the case of the high current density specimens, some hole formation was observed towards the end of the tests, indicating the presence of sufficient stress to fracture the films after the occurrence of appreciable thinning. Although it may be concluded that plating at low current density increases the subsequent electrode life, presumably by decreasing stress, it may not be practical to take this approach too far. At 4 mA cm^{-2} a 100 C ($\simeq$ 130 μm) plating takes about 7 h to complete.

6. Redeposition

As pieces of lead dioxide are lost from the elec-

trode they react with the electrolyte to produce lead sulphate, and the saturation concentration of lead ions is soon reached. The possibility then exists that lead dioxide may be redeposited, and the structures so formed were examined by electron microscopy. The original surface (Fig. 2f), which is a dark metallic grey consisting of sharply defined pyramidal blocks, is converted to a fragmented structure covered with amorphous growths of lead dioxide (Fig. 2g), and the colour of the electrode changes to a light brown. As the layer thins the angular nature of the crystals at the solution interface is soon lost. On the other hand redeposition at the bottom of a hole may be relatively uninterrupted by thinning, and dendritic formations are usually well developed (Fig. 2h). The holes then appear to be much darker in colour than the surrounding bulk oxide. The observations suggest that freshly exposed titanium does not become passivated under these circumstances, even when in contact with the solution at high applied potentials. Possibly the residual lead dioxide affords a degree of anodic protection, and the build up of a resistive titanium oxide layer is not the primary cause of electrode failure.

After considerable thinning, large areas of substrate, especially at the edges of the specimen, become exposed, and spherical nuclei of redeposited lead dioxide consisting of many small crystallites (Figs. 2 i and j) may be observed. They are quite different in appearance from the nuclei of the original layer, shown in the previous paper [1], and are often charged up by the electron beam, an indication of poor electrical contact with the substrate. The titanium, therefore, may be partially passivated in these areas.

Occasionally pieces of the lead dioxide layer may be partially detached in such a manner that conversion to lead sulphate can take place. The resulting crystals, which are quite distinctive, are shown in Fig. 2k.

The rate of redeposition may be calculated from the dimensions of the cell, and the known flow rate, by using the empirical relationships given by Pickett and Ong [3] for similar configurations. For developed turbulent flow, assuming a lead ion concentration in solution of 1.4×10^{-4} mol dm^{-3} [4] (i.e. the saturation value in water), one obtains a limiting rate of about 0.18 mg cm^{-2} h^{-1}. This value must be multiplied by a parameter representing the enhancement of mass transfer due to gas evolution. The paper of Janssen and Hoogland [13] suggests that the appropriate factor may be as high as 10 for oxygen evolution at 1 A cm^{-2} but falling towards unity as the current density decreases. Hence a maximum redeposition rate of 2 mg cm^{-2} h^{-1} can be predicted. If the solubility of lead sulphate in sulphuric acid was used in the calculations, lower values would be obtained. The amounts derived in this way are much less than the observed thinning rates, as would be expected.

7. Thinning

In addition to the material removed by the initial formation of holes all specimens gradually lose weight during testing, and the lead dioxide layer thins visibly, often until less than 10% remains at failure. Most electrodes were weighed at the end of their useful lives, but in a few cases the thinning was followed in more detail by obtaining several intermediate readings. The data are presented by plotting weight loss against total charge passed up to the time of each removal from the cell. From Fig. 6, which refers to specimens plated at 60° C, the following relationship is obtained,

$$dl/dt = -\lambda i \qquad (9)$$

where l is the oxide thickness or mass per unit area, and λ is a constant for each electrode. The initial steep rise shown by electrode 91 is due to shedding, which was absent in the other examples. The intermediate and end points of 18 further specimens (not shown) are all located in the sector defined by curve 91 and the dashed line below curve 96, and the parameter λ varies between 0.40 and 0.84 μgC^{-1}. There is some correlation between λ and the expected level of electrodeposition stress. For example, specimen 96 was a low current density plating, implying low stress, and specimen 91 was highly stressed, as indicated by the initial shedding.

Possible mechanisms of the thinning process may now be considered in terms of the current density dependence expressed in Equation 9. Kuhn [4] has suggested that the fluctuations caused by the masking effect of gas bubbles would be sufficient to lower the potential at appropriate

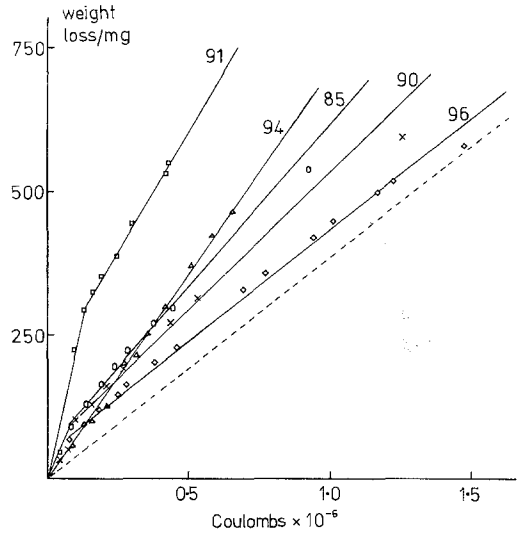

Fig. 6. Weight loss as a function of total charge passed in oxygen evolution.

places to values at which lead sulphate could be formed. Dissolution would then take place. This theory is unsatisfactory in view of the large potential drops which would be required, and, furthermore, high thinning rates would be expected at low current densities and potentials whereas the opposite dependence is observed experimentally. Also, as pointed out previously, the calculated limiting transport rates for Pb^{2+} in solution are always less than the observed thinning rates. If an electrochemical mechanism is to be assumed, then the kinetics would be more in favour of a dissolution process involving a higher valency lead species, e.g. Pb^{VI}. However, no such entity has been reported.

An alternative explanation, based on the previously suggested model for the lead dioxide layer, may be more satisfactory. Since both the overpotential and the current density are high, in the present circumstances, considerable power dissipation from the reaction resistance may be anticipated, and there will be a temperature rise at the solution interface. Roark [11] has indicated that a clamped plate treated in this way is subject to local stress on the heated face, and by analogy, the lead dioxide must be similarly affected. The masking of parts of the surface by gas bubbles will enhance the stress at other places by momentarily concentrating the current density, and the possibility of exceeding the critical stress exists. Cracking will then develop and small pieces of lead dioxide will be continually removed.

8. Current time behaviour

Since the thinning exposes fresh surfaces to the solution, the observed decay of the rate of the oxygen evolution reaction must be the result of a deactivation process. The current density drops slowly at first and then abruptly just before failure and a transition time may be measured. A logarithmic time base has been used for convenience in Figs. 7–10. Although the lifetimes are prolonged, as might be expected, by increasing the initial thickness of the deposit, the effects of other variables are less easily assessed. Any proposed model should include rate equations which enable the time behaviour of both the current density and the layer thickness to be predicted. Three possibilities are discussed below.

8.1. *Solution deactivation*

The electrode is assumed to be poisoned by the adsorption or electrodeposition of impurities from the solution, so that at a given time only a fraction, θ, of the surface remains active. The redeposition process could be an example of a deactivating reaction if the particles were in poor electrical contact with the bulk oxide. In the simplest case the current density and the poisoning rate are both directly proportional to the active area, and reactivation takes place by thinning from the inactive sites, $1-\theta$, to give the rate equations:

$$i = k_4\theta \tag{10}$$

$$\text{Rate of poisoning} = k_5\theta \tag{11}$$

$$\text{Rate of reactivation} = k_6(1-\theta)\theta. \tag{12}$$

Equation 12 also involves the dependency of thinning on current density, described previously in Equation 9. It follows that

$$\mathrm{d}\theta/\mathrm{d}t = k_6(1-\theta)\theta - k_5\theta \tag{13}$$

and integration gives the time variation of θ. The result predicts an exponential decay of the current at long times, without a transition, which is not in accord with experiment.

Other objections to the model may be stated.

Thus, most impurities would be desorbed rather than adsorbed at the high anodic potentials encountered, and the specific inhibition of oxygen evolution, for example, by a Kolbe type reaction is unlikely. Furthermore, the time constant for surface coverage by transport from the solution would be much shorter than that observed, i.e. of the order of minutes rather than hours or days.

8.2. *Actives sites model*

Suppose that the oxygen evolution reaction takes place only at certain active sites, which are slowly removed at the solution interface and replaced by diffusion from the bulk material. The equation of transport is

$$D\frac{\partial^2 v}{\partial x^2} = \frac{\partial v}{\partial t} \tag{14}$$

where v is the concentration of active material, D is the diffusion coefficient and x the distance from the substrate. At the solution interface, where the observed current depends directly on v, let the rate of removal of activity be proportional to the surface concentration. Then one has

$$\text{at } x = l \qquad i = k_7 v \tag{15}$$

and

$$\text{at } x = l \qquad D\frac{\partial v}{\partial x} = -hv. \tag{16}$$

Here h is a constant and Equation 16 corresponds to the 'radiation boundary condition' of Carslaw and Jaeger [14]. Other boundary conditions are:

$$v = V \qquad \text{at } t = 0 \qquad \text{for all } x$$

and

$$D\frac{\partial v}{\partial x} = 0 \qquad \text{at } x = 0. \tag{17}$$

The above authors have discussed the solution of these equations and have presented diagrams showing the surface values of v. The treatment must now be extended by taking into account the thinning reaction, which gives the further boundary conditions

$$\frac{\mathrm{d}l}{\mathrm{d}t} = -\lambda v \qquad \text{at } x = l$$

and

$$l = L \qquad \text{at } t = 0. \tag{18}$$

Solutions have been computed at this laboratory by Hodgkins in terms of the dimensionless variables

$$y = \frac{x}{L}, \quad s = \frac{l}{L}, \quad \psi = \frac{v}{V} \quad \text{and} \quad \tau = \frac{Dt}{L^2}. \tag{19}$$

Surface values of the parameter ψ represent the ratio of the current at a given time to the initial current. The working equations are then

$$\frac{\partial^2 \psi}{\partial y^2} = \frac{\partial \psi}{\partial \tau} \tag{20}$$

with

$$\left.\begin{aligned} &\frac{\partial \psi}{\partial y} = 0 \qquad \text{at } y = 0 \\ &\frac{\partial \psi}{\partial y} = -\frac{hL}{D}\psi = -A\psi \qquad \text{at } y = s \\ &\frac{\partial s}{\partial \tau} = -\frac{\lambda L V}{D}\psi = -B\psi \qquad \text{at } y = s \\ &\psi = 1 \quad \text{for all } x \quad \text{and } s = 1 \quad \text{at } \tau = 0. \end{aligned}\right\} \tag{21}$$

From these definitions it follows that, for a given initial layer thickness, A relates primarily to the deactivation constant h and in turn to the polarization voltage or the initial current density, and B is determined by the thinning rate constant λ. The calculations show how the current parameter, ψ, depends on A and B. Firstly, at constant A, the initial current decay is retarded by increasing B, but the final abrupt drop is more pronounced and electrode life is diminished. Secondly, with B constant, the plateau like shape of the decay is progressively removed by increasing A, but lifetimes are not significantly reduced until A becomes greater than B.

The experimental results conform to these trends. Fig. 7, for example, shows the polarization behaviour of a batch of specimens with initial layer thicknesses 10 μm (approximately), which were plated together but tested at different voltages and initial current densities, in other words at constant B with varying A. The lines drawn through the points were calculated from the model. Somewhat surprisingly the polarization conditions do not greatly affect the times to failure. The data fit quite well with $B = 0.2$ and A decreasing from 0.4 to 0.01 as the initial current density is reduced. $\tau = 1$ is at 1.5 h.

A similar set of decays for electrodes with ten times thicker lead dioxide layers (approximately

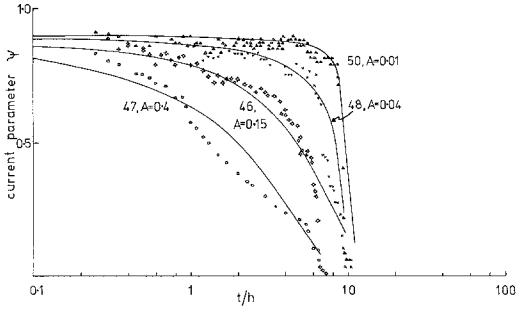

Fig. 7. Experimental current decays for 10 μm layer specimens. The curves were calculated with $B = 0.2$, $\tau = 1$ at 1.5 h, and various values of A. Initial current were: 47 at 4.0 A; 46 at 2.8 A; 48 at 2.0 A; 50 at 1.0 A.

100 μm) is given in Fig. 8. Here $B = 2$, $0.8 < A < 1.8$ and $\tau = 1$ is in the region of 150 h. Examination of Equations 21 demonstrates the compatibility of the two groups of experiments, since a tenfold increase in L should increase A and B by the same factor, and should also shift the $\tau = 1$ position along the time axis by two decades. All electrodes with $L = 100\,\mu$m are covered by the range $0.7 < B < 2.2$ in agreement with the variation in λ of Fig. 6. Since, in many instances the initial conditions of testing were fairly constant, most of the curves are fitted by $1 < A < 2$, although values as high as 4 and as low as 0.5 were encountered.

With the appropriate choice of A and B the model provides a good fit to many of the experimental curves, as in Fig. 9, but some electrodes show a more or less pronounced two-stage decay, as illustrated. This is especially the case when plating is performed at 60° C in the presence of CTAB. Possibly a structure with inner and outer layers of different properties is indicated.

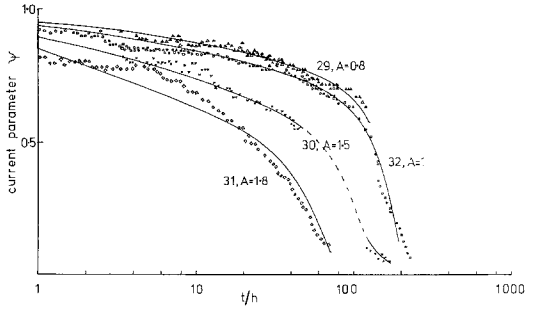

Fig. 8. Current decays for 100 μm layer specimens. The curves were calculated with $B = 2$, $\tau = 1$ distributed around 150 h, and various values of A. Initial currrents were: 29 at 2.5 A; 32 at 3.5 A; 30 at 5.0 A; 31 at 6.0 A.

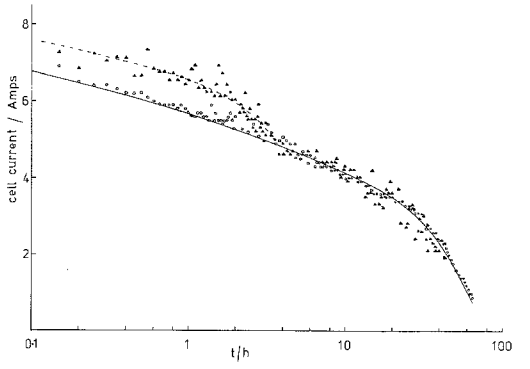

Fig. 9. Current decays for 100 μm specimens. Electrode 66 (○) from the acetate series, illustrates the fit of the experimental points to the solid curve calculated with $A = 2$ and $B = 2$. Electrode 84 (△) from the CTAB series shows a typical double wave decay.

The complete solution of the differential equations also enables the time behaviour of s, the oxide thickness parameter, to be calculated. In Fig. 10 both the current and the thickness decay for electrode 96 are matched by the computations, using the same constants for both curves. Other 100 μm specimens, weighed at intervals, show a similar behaviour with A and B confined to a narrow range. The model shows, moreover, that the decay in s should lag behind that of ψ for the 10 μm specimens of Fig. 7. This was born out in practice, since the electrodes had lost less than 20% of their original weights at failure, and most of this was due to hole formation.

In conclusion some speculation as to the nature of the active sites in the model may be offered. It is possible, for example, that they correspond to Pb^{3+} ions in the non-stoichiometric PbO_2. This was postulated by Sunderland [15] to explain

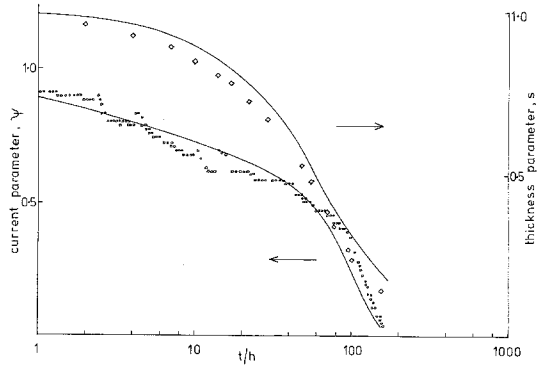

Fig. 10. Time decay of current, ψ, and thickness, s, parameters for electrode 96. The curves were calculated with $A = 1.5$, $B = 2$ and $\tau = 1$ at 150 h.

anomolous peaks in cyclic voltammetry studies on lead electrodes. Enhanced activity of ions of unusual valencies has been suggested before in connection with other oxide anodes such as nickel and silver [16].

8.3. *Oxide growth model*

It has been maintained [4] that titanium based anodes fail because the substrate gradually oxidizes and introduces a highly resistive element into the current path, but the resulting kinetic behaviour has not been previously investigated theoretically in any detail. An approach to the problem will be outlined here by considering firstly, the transport of reacting material and the relevant oxide growth law, and secondly the relationship between titanium dioxide thickness and electron current density.

Since movement through either oxide may be rate controlling then: (a) if ionic transport through the TiO_2 is limiting, the growth kinetics should be similar to those of direct anodic passivation, and a logarithmic, inverse logarithmic or parabolic law could follow, depending on the oxide thickness and properties [17]. This assumes that the voltage is dropped entirely across the TiO_2 layer, which may be approximately true in the later stages. (b) When ionic movement through the PbO_2 is slow, which seems more likely in view of the relative oxide thicknesses, then the previously described diffusion equations may be used with modified boundary conditions. At the TiO_2/PbO_2 interface one could assume either the 'radiation boundary' condition, or zero concentration, noting that at long times the two become equivalent. At the solution interface the reactant concentration may be maintained constant, or may be allowed to decay from an initial value. The former corresponds to the continuous generation of, say, O^{2-} ions, which then diffuse across the PbO_2 towards the reaction zone, and the latter to a direct reaction with the PbO_2 itself. If, on the other hand, slow product species (excess lead ions, for example) diffuse away from the reaction zone, at the TiO_2/PbO_2 boundary, towards the solution, it can easily be shown that the kinetic conditions are equivalent to those just mentioned, the only difference being a change in diffusion coefficient. The model as it stands is similar in many ways to that of the active sites concept, and could be solved [14] to give the total quantity, Q, of diffused reactant, and hence the TiO_2 growth, as a function of time. However, when the thinning process is introduced difficulties arise, because it becomes necessary to assume a relationship between current density (and hence thinning rate) and Q. This point will be discussed shortly. (c) It is possible that the PbO_2 is porous, and the titanium substrate is passivated by direct contact with the solution. This situation should produce results similar to that just described, after allowing for a suitable change in diffusion coefficient. However, as implied earlier, this case is considered to be unlikely because passivation does not seem to occur until large areas are exposed, and because the time constant of a solution diffusion process should be much less than that observed.

The derivation may now be extended to include the electronic current, i, which enters the model in two ways, firstly in its dependency on Q, and secondly in its affect on the thinning process. Allard and Heusler [18] have suggested that $\log i$ depends on the field strength in the TiO_2, so that one has

$$\log i = \log k_8 + k_9 \frac{Z}{Q} \qquad (22)$$

where k_8 and k_9 are constants, and Z is the voltage across the oxide. However, it is not clear to which film thicknesses this equation applies, and a rate based on considerations of electron tunnelling would be more appropriate at the lower values of Q. In practice the oxide is probably in a transition region between the two cases, and, in the absence of detailed experimental work, it is not possible to make the required transformation from $Q(t)$ to $i(t)$. Even if a practical relationship between i and Q were available it would be necessary to assume an initial TiO_2 thickness. An approximation could be attempted by neglecting the thinning reaction and then using Equation 22, however, the result would seem to indicate a wavelike decay of $\log i$, rather than i, which is not particularly satisfactory. Similarly, when transport across the TiO_2 is limiting, $\log i$ would be proportional to $1/\log t$ or $t^{1/2}$, again not in accord with practice.

Apart from the apparently good fit of the data to the predictions of the active sites model, another argument in its favour, when compared

to the oxide growth theory, is to be found in the experiments interrupted at intervals. Always, on reinsertion into the cell, the current increases over the prior value before decaying back to the original curve. If oxide growth were limiting the opposite behaviour would be expected, since the TiO_2 layer could not have thinned during the removal period. Indeed further oxidation by direct reaction with PbO_2 could well occur upon storage. This evidence, and the absence of any apparent effect of electrode age, before initial use, on performance, therefore, contradicts the resistance model. The increased activity is simply explained, on the other hand, as an outwards diffusion of sites towards the surface region, which has been depleted during polarization.

9. Conclusions

(a) The breakdown of oxygen evolving PbO_2/Ti anodes in sulphuric acid solution occurs by three processes, shedding, thinning and deactivation.

(b) Shedding, i.e. the formation of holes in the PbO_2 layer, results from the catastrophic relief of stresses produced during electrodeposition and subsequent usage. The effect of layer thickness on the diameters and numbers of holes has been explained by a buckling plate model.

(c) Thinning is the result of thermal stress generated at the solution interface.

(d) Attempts have been made to reduce stress by manipulation of the plating bath. High temperature and low current density operation are more successful than the use of additives.

(e) The activity of the electrodes decays with time. The process has been modelled in terms of the diffusion of active material from the bulk PbO_2. Alternative models have also been considered.

(f) Lead dioxide is continually redeposited on the electrodes by oxidation of lead ions from the solution.

Acknowledgements

Thanks are due to A. McKay and J. Noakhes for experimental participation. R. Hodgkins computed solutions to the diffusion equations.

References

[1] D. Gilroy and R. Stevens, *J. Appl. Electrochem.* **10** (1980) 511.
[2] A. P. King, Electricity Council Research Centre, Report M1134 (1978).
[3] D. J. Pickett and K. L. Ong, *Electrochim. Acta* **19** (1974) 875.
[4] A. T. Kuhn, 'The Electrochemistry of Lead', Academic Press, London (1979).
[5] N. Pangarov and R. Pangarova, *J. Electroanal. Chem.* **91** (1978) 173.
[6] K. S. A. Gnanasekaran, K. C. Narasimham and H. V. K. Udupa, *Electrochim. Acta* **15** (1970) 1615.
[7] S. Vasundara, K. C. Narasimham and H. V. K. Udupa, *ibid.* **16** (1971) 1301.
[8] K. C. Narasimham, S. Vasundara and H. V. K. Udupa, *Can. J. Chem.* **53** (1975) 3327.
[9] C. J. Bushrod and N. A. Hampson, *Br. Corros. J.* **6** (1971) 129.
[10] A. T. Kuhn and R. B. Lartey, *Corrosion – NACE* **33** (1977) 73.
[11] R. J. Roark, 'Formulas for Stress and Strain', 4th edn, McGraw-Hill, New York (1965).
[12] S. Timoshenko, 'Strength of Materials, Part II', 3rd edn, Van Nostrand, Princeton (1956).
[13] L. J. J. Janssen and J. G. Hoogland, *Electrochim. Acta* **15** (1970) 1013.
[14] H. S. Carslaw and J. C. Jaeger, 'Conduction of Heat in Solids', 2nd edn, Oxford (1959).
[15] J. G. Sunderland, *J. Electroanal. Chem.* **71** (1976) 341.
[16] B. E. Conway, M. A. Sattar and D. Gilroy, *Electrochim. Acta* **14** (1969) 677.
[17] A. K. Vijh, 'Electrochemistry of Metals and Semiconductors', Marcel Dekker Inc., New York (1973).
[18] K. D. Allard and K. E. Heusler, *J. Electroanal. Chem.* **77** (1977) 35.